HHS Public Access

Author manuscript

J Drug Deliv Sci Technol. Author manuscript; available in PMC 2022 February 01.

Published in final edited form as:

J Drug Deliv Sci Technol. 2021 February ; 61: . doi:10.1016/j.jddst.2020.102128.

Theophylline-nicotinamide pharmaceutical co-crystals generated using hot melt extrusion technology: Impact of polymeric carriers on processability

Priyanka Srinivasan[a], **Mashan Almutairi**[a], **Nagireddy Dumpa**[a], **Sandeep Sarabu**[a], **Suresh Bandari**[a], **Feng Zhang**[c], **Eman Ashour**[a], **Michael A. Repka**[a,b,*]

[a]Department of Pharmaceutics and Drug Delivery, School of Pharmacy, The University of Mississippi, University, MS, 38677, USA

[b]Pii Center for Pharmaceutical Technology, The University of Mississippi, University, MS, 38677, USA

[c]College of Pharmacy, The University of Texas at Austin, TX, 78712, USA

Abstract

The objective of the current study was to develop theophylline (TPH) nicotinamide (NAM) pharmaceutical co-crystals using the hot melt extrusion (HME) technology and evaluate the processability of the co-crystals using different polymeric carriers. A physical mixture of 1:1 M ratio of TPH and NAM was employed to prepare the co-crystals. Hydroxypropylmethylcellulose acetate succinate, polyethylene oxide, and Kollidon® VA-64 (5% w/w) were investigated as polymeric carriers for the HME process. Solid-state characterization using differential scanning calorimetry showed two endothermal peaks, one at 126.4 °C indicating eutectic formation and another at 174 °C indicating the melting point of the co-crystal for all formulations, except the Kollidon® VA-64 extrudates, which showed a single peak at 174 °C. Fourier-transform infrared spectroscopy and powder X-ray diffraction studies revealed the formation of co-crystals. The feasibility to formulate the extrudates into solid dosage forms was assessed by formulating a tablet blend. The three-month stability studies showed no degradation at the accelerated stability conditions of 40 (±2) ° C and 75 (±5) % RH. Finally, the results demonstrated that the presence of mixing zones in screw configuration and extrusion temperature are critical processing parameters that influence co-crystal formation.

*Corresponding author. Department of Pharmaceutics and Drug Delivery, School of Pharmacy, The University of Mississippi, University, MS, 38677, USA., marepka@olemiss.edu (M.A. Repka).

CRediT authorship contribution statement

Priyanka Srinivasan, Suresh Bandari, Michael A.Repka conceptualized the study.Priyanka Srinivasan, Mashan Almutairi, Nagireddy Dumpa, Sandeep Sarabu investigated the study. Feng Zhang provided resources and performed XRD analysis. Formal Analysis was done by Feng Zhang and Eman Ashour.Writing-Original Draft by Priyanka Srinivasan. Writing-Review and Editing was done by Suresh Bandari and Michael A.Repka. Supervision was done by Michael A.Repka.

Declaration of competing interest

The authors declare that they have no known competing financial interests or conflicts of interest or personal relationships that could have appeared to influence the work reported in this paper.

Keywords

Co-crystal; Theophylline; Nicotinamide; Kollidon VA 64; Hot melt extrusion

1. Introduction

The hot melt extrusion (HME) technology has been well established for the mixing, compounding and processing of materials in the plastic, rubber, and food industries. However, in the early 1970s, the use of HME became prevalent in the pharmaceutical sector. In fact, it was widely used as a manufacturing tool in formulation and product development [1]. HME has been used in the manufacture of different dosage forms and formulations, including granules, tablets, pellets, implants, ointment, films, transdermal systems, and several advanced applications such as taste masking, abuse deterrent, and targeted drug delivery [2–9]. HME is a continuous pharmaceutical process where the input materials are pumped into the extruder at temperatures above the glass transition temperature (T_g) and melting temperature (T_m) to obtain molecular-level mixing of the materials [1]. Processing parameters such as temperature, feed rate, and screw speed play an important role in the extrusion process as they affect the final quality of the product. The major advantage of using the HME is it is a solvent free process, which provides better inline monitoring, automation, easy scale up, and significant reduction in capital and labor costs [10,11]. There are however a few drawbacks and challenges during the extrusion process such as high energy input from the applied shear forces and high temperature that could impact the quality of the extruded product [12].

Recently, the pharmaceutical industry has been focusing on modifying the existing drug molecules rather than developing a new chemical entity (NCE) [13]. An important criterion in pharmaceutical-drug development is increasing the solubility of a drug while maintaining its stability. Some of the most common approaches to overcome solubility and bioavailability issues include process modifications such as drug micronization and preparing amorphous solid dispersions. More recently, chemical transformations such as salt or co-crystal formation have garnered interest in improving the physicochemical properties of the Active Pharmaceutical Ingredients (API) [14].

Specifically, the co-crystallization of active pharmaceutical ingredients (API) has expanded in recent times, which involves modifying the physiochemical properties of drug substances to improve solubility, stability, flowability, and compressibility. Pharmaceutical industries mainly prefer the crystalline forms of active compounds owing to the inherent stability of crystalline materials. The API, regardless of the acidic, basic, or ionizable groups present in its core, is co-crystallized, which is a unique feature of co-crystallization [15]. A crystalline complex of two or more molecules is formed during co-crystallization, which is an API with a pharmaceutically acceptable “Generally Regarded As Safe” (GRAS) co-former, bonded together non-covalently via hydrogen bonding in the crystal lattice [16]. Excipients, different drug molecules, or a solubilizing agent can be chosen as a co-former with an API to result in a pharmaceutically acceptable co-crystal [17]. Co-formers act as a guest molecule, thereby enhancing the physiochemical properties of APIs without altering the structure and

pharmacology of the drug molecule during intermolecular interactions [18]. Intermolecular interaction and hydrogen bonding are important characteristic features of a co-crystal [15]. Co-crystals exhibit different physical properties compared to their corresponding pure components [19]. Conventionally, co-crystals are prepared by slow evaporation, neat grinding, liquid-assisted grinding, melt crystallization, sublimation, and solution crystallization. Solution crystallization has proven to be a practical and scalable process owing to its ease in reproducibility, phase control, and particle size control. However, there are some drawbacks with respect to solution crystallization as it involves solvents and an understanding of ternary phase diagrams related to the co-crystal constituents and the solvent, which is laborious and time consuming. Recently, the HME technology has been investigated for use in co-crystal formation as it is a solvent-free scalable technique that is easily amenable to quality by the design (QbD) approach [20–22]. However, processability is a key factor in the formation of co-crystals using the HME process.

The main objective of the current investigation was to develop theophylline (TPH) nicotinamide (NAM) pharmaceutical co-crystals using the HME technology and evaluate the processability of the cocrystals by using different polymeric carriers. TPH, a methylxanthine derivative used for the treatment of respiratory disorders such as asthma was selected as the API. TPH is reported to have four anhydrate polymorphs and a monohydrate form. NAM, a member of the vitamin B family that was selected as the co-former for the formation of co-crystals, exists as four polymorphs [23]. TPH (M.P. 273 °C) was selected as a model API to investigate the processability of high melting point API using HME and the impact of polymer matrix in the formation of stable co-crystals. Matrix assisted co-crystallization enhances the physical and chemical stability of co-crystals and involves the co-processing of the drug and co-former with polymers [24]. A pharmaceutical grade thermoplastic polymer is used in the extrusion process for the manufacture of co-crystals [25]. The selection of a matrix material plays an important role in the extrusion process of co-crystal production as it aids in improved flowability, compaction, and drug-release kinetics of the final product [26,27]. Polymeric carriers such as HPMCAS-MG, PEO N80, and Kollidon® VA-64 with varying properties at a concentration of 5% (w/w) were examined as the matrices.

2. Materials and methods

2.1. Materials

Pure TPH Anhydrous and NAM were purchased from Sigma-Aldrich, Inc. (St. Louis, MO, USA) and used as received. Aquasolve™ hydroxypropylmethylcellulose acetate succinate (HPMCAS-MG grade) was obtained from Ashland Inc. (Covington, KY, USA). PEO N80 was obtained from Colorcon Inc. (Harleysville, PA, USA). Kollidon® VA-64 was obtained from BASF-SE (Ludwigshafen, Germany). The chemical reagents and solvents used in this study were purchased from Fisher Scientific (Fair Lawn, NJ, USA) and were of analytical grade.

3.1. Methods

3.1.1. Hot melt extrusion—TPH and NAM in a 1:1 M ratio equivalent to 50g were weighed and blended thoroughly using a twin shell V-blender (Globe Pharma, Maxiblend®)

for 15 min. Co-crystallization was carried out using a 11-mm co-rotating twin-screw extruder (Process 11 Twin Screw Extruder, Thermo Fisher Scientific) with a customized screw design of four mixing zones employing several mixing elements as shown in Fig. 1. The prepared blend was fed into the extruder hopper and operated without a die. The extrusion was performed with a 2 mm rod-shaped die when 5% (w/w) of the polymeric carriers were incorporated as the matrix material in the study. The processing temperature studied was in the range of 140–170 °C at a screw speed of 50 rpm. The compositions of different formulations F1–F7 is mentioned in Table 1.

3.2. Solid state characterization

3.2.1. Differential scanning calorimetry (DSC)—The thermal behavior of the physical blend and the extruded formulations was examined using DSC (DSC 25 Discovery series, TA instruments) coupled with a refrigerated cooling system and equipped with the Trios manager software. The accurately weighed samples (5–8 mg) were hermetically sealed in an aluminum pan and heated from 25 °C to 300 °C at a heating rate of 10 °C/min. Ultrapure nitrogen at a flow rate of 50 mL/min was used as the purge gas.

3.3. Fourier-transform infrared spectroscopy (FTIR)

The spectra of pure TPH, pure NAM, polymeric carriers, physical mixtures, and the corresponding extrudates were determined using FTIR (Agilent Technologies Cary 660, Santa Clara, CA). The bench was equipped with an ATR (Pike Technologies MIRacle ATR, Madison, WI) that was fitted with a single bounce diamond-coated ZnSe internal reflection element. The scanning range was 400–4000 cm^{-1}.

Powder X-Ray Diffraction (PXRD).

The crystallinity of pure TPH, pure NAM and the extrudates were examined by using a PXRD apparatus Rigaku X-ray system (D/MAX-2500PC, Rigaku Corp., Tokyo, Japan) using Cu rays with a voltage of 40 kV and a current of 40 mA, over a 2θ scanning range of 2°–50°, with a step width of 0.02°/S and a scan speed of 2°/min.

3.4. Scanning Electron Microscopy (SEM)

The morphological characteristics of pure TPH, pure NAM, and the extrudates were examined using a JSM-7200 FLV Field Emission Scanning Electron Microscope (JOEL, Peabody, MA, USA) operated at an accelerating voltage of 5 kV. All the samples were placed on the SEM stubs and adhered by using double-adhesive tape. The samples were sputter-coated with Platinum under an argon atmosphere using a fully automated Denton Desk V TSC Sputter Coater (Denton Vacuum, Moorestown, NJ, USA) prior to imaging.

3.5. Particle size distribution

The milled extrudates were evaluated for particle size distribution by sieve analysis using a vibratory shaker (Performer III SS-3, Gilson Inc.) The method was carried out by sifting the powder sample using a stack of pre-weighed sieve nest combination of #30,40,60,80,120 and 200 ASTM mesh series. A quantity of 5g of sample was placed into the sieve nest and the study was performed for 10 min at an amplitude of 5 with a tapping rate of 60 taps/min.

The retained amount of powder on each sieve was accurately weighed after the analysis. Particle size distribution plots were schemed out based on the weight distribution [28].

3.6. Pharmaceutical characterization

Carr's Compressibility Index and Hausner's Ratio.

The flow characteristics of pure TPH and the TPH-NAM extrudates (co-crystals) were predicted using Carr's compressibility index and Hausner's ratio [9].

$$\text{Carr's index} = 100 \text{ x } \frac{\text{Tapped density} - \text{Bulk density}}{\text{Tapped density}}$$

$$\text{Hausner's ratio} = \frac{\text{Tapped density}}{\text{Bulk density}}$$

3.7. Loss on drying

The moisture analyzer (MB 45, Ohaus) was employed to investigate the moisture content of pure TPH and TPH-NAM co-crystals by measuring the uptake and loss of vapor. The sample was weighed, heated, dried, and re-weighed (each experiment was carried out in triplicate). The weight after drying was subtracted from the initial weight and the loss of moisture was determined based on the loss in mass.

3.8. In vitro dissolution study

Dissolution studies of pure TPH and the pure co-crystals, tablet physical blend, and compressed tablet were assessed using USP type II paddle method in an.

SR8-plus Hanson dissolution apparatus (Hanson SR8-plus™; Hanson Research, Chatsworth, CA, USA). TPH-NAM extrudates, physical blend, tablet, and co-crystal equivalent to 100 mg of pure TPH were added to 900 mL of water in each dissolution vessel (n = 3). The temperature of the medium was maintained at 37 ± 0.5 °C and the paddle rotation was set to 50 rpm. Approximately 2 mL of samples was withdrawn at 5, 15, 30, 45, and 60 min intervals, filtered using a 0.2 μm (Millex® GV, Durapore® PVDF) filter, and analyzed using HPLC.

3.9. High-performance liquid chromatography (HPLC)

Quantitative HPLC was performed as reported in the USP 38, on an isocratic high-performance liquid chromatograph (Waters Corp., Milford, MA, USA) equipped with an auto sampler, UV/VIS detector, and Empower software. TPH was analyzed on a Phenomenex Luna C18 column (5 μm, 250 mm × 4.6 mm), at a detection wavelength of 280 nm. The composition of the mobile phase was 92:7:1 (% v/v/v) 0.01 M sodium acetate trihydrate buffer: acetonitrile: glacial acetic acid. The flow rate was set to 1 mL/min. The samples were filtered through a 0.2-μm filter (Millex® GV, Durapore® PVDF) before being injected into the column (10 μL). The calibration curve was plotted by varying the standard solution concentration from 10 to 70 μg/mL [9].

3.10. Stability studies

A stability study for the F4 and F7 formulations was performed using the Caron 6030 stability chamber for three months. Formulations were stored in HDPE vials at 40 (±2) ° C/75 (±5) % RH. The formulations were evaluated at specific time intervals to derive their physical characteristics. DSC was also performed to understand the thermal behavior of co-crystal after stability.

4. Results and discussion

4.1. Hot melt extrusion

HME was performed to generate TPH NAM co-crystals and assess the processability during co-crystal formation via the incorporation of polymeric carriers such as HPMCAS-MG, PEO N80, and Kollidon® VA-64. The extrusion process was carried out using the Process 11 Twin screw extruder. The customized screw configuration with four mixing zones employed in this study was tailored for high mixing capacity and longer residence time to achieve complete co-crystal formation. In preliminary experiments, extrusion was performed at lower temperatures ranging from 110 to 150 °C. These observations revealed that cocrystals were not formed at lower processing temperatures. The extrusion trials carried out at higher temperatures revealed that co-crystal formation was complete at 170 °C compared to extrusion at 160 °C. The experiment clearly suggested that the customized screw design and increased temperatures enabled efficient mixing in the extruder barrel and created a new surface contact, thereby continuously promoting cocrystal formation [20]. Thus, the formation of the co-crystal at the extrusion temperature near the M.P. of co-crystal was aligned with the data from previous reports (Fig. 2) [20]. Besides temperature, the screw speed played an important role in co-crystal formation. The screw speed was varied from 25 to 100 rpm; it was assumed that with lower screw speeds, the residence time in the extruder increased, which lead to complete co-crystal formation [20]. Hence, a screw speed of 50 rpm was selected as the optimal screw speed with acceptable torque. Further, HME was performed by co-processing the drug and the co-former in the presence of the polymeric carriers HPMCAS-MG, PEO N80, and Kollidon® VA-64, at a concentration of 5% w/w. Individual polymeric carriers along with equimolar quantities of drug and co-former in a 1:1 M ratio were blended and extruded using a 2-mm rod shaped die at the end of the barrel. The extrusion was performed using a tailored screw design and processed at barrel temperatures of 160 and 170 °C with a screw speed of 50 rpm. The co-crystal formed was embedded in the matrix material and solidified upon exiting the extruder. The co-crystals were collected in the form of rod shaped extrudates. The processing conditions such as extrusion temperature, screw speed, and observed torque values are shown in Table 1. The torque (%) in Table 1 demonstrates relatively higher torque values with an increase in temperature from 140 °C to 170 °C; this may be attributed to the softening/partial melting of the co-crystal form (M.P. 174 °C). Nevertheless, the impact of the polymer in the processability of the extrusion for co-crystal formation was clearly evident by the decreased torque (%) in the polymer-assisted formulations. The Kollidon® VA-64 based formulation displayed complete conversion into the co-crystal form with a low torque value at 160 °C, suggesting improved processability among the polymers investigated.

4.2. Solid state characterization

4.2.1. differential scanning calorimetry—Differential Scanning Calorimetry performed on all formulations including pure TPH, pure NAM, the corresponding physical mixture, extrudates, and the formulations with 5% w/w of HPMCAS-MG, PEO N80, and Kollidon® VA-64 revealed the impact of polymeric carriers during the processing of formulations and their influence on thermal properties. Pure TPH and pure NAM showed melting peaks at 273 °C and 129 °C, respectively. The DSC thermograms of the physical mixtures showed the presence of two characteristic endothermal peaks, the first at the same temperature as the melting peak of NAM (126.4 °C) and another new co-crystal peak at (174 °C) (Fig. 3). Specifically, the thermograms of the extrudates revealed the presence of a low intense endothermal peak at ~126.4 °C, which decreased and finally disappeared at 160 °C (extrusion temperature) with the Kollidon® VA-64 extrudates. The Kollidon® VA-64 extrudates demonstrated a single characteristic co-crystal peak at 174 °C. A characteristic melting endotherm at 174 °C, which differed from the melting points of either TPH (273 °C) or NAM (129 °C), indicated the formation of a new phase between TPH and NAM during HME. This was in accordance with the previous report of TPH-NAM co-crystal using the co-grinding method [17]. DSC thermograms of the co-crystals with HPMCAS-MG and PEO N80 as polymeric carriers exhibited similar thermal profiles as those of the extruded TPH NAM co-crystals. However, eutectic formation at 126.4 °C was not observed in the Kollidon® VA-64 assisted co-crystals, that may indicate complete co-crystal formation during HME.

4.3. Fourier transform infrared spectroscopy

Fourier transform infrared spectroscopy analysis was performed to determine the potential interactions between the drug, co-former, and polymeric carriers (Fig. 4). TPH contains two carbonyl groups, which are observed at 1662 cm^{-1} and 1706 cm^{-1} while NAM shows characteristic peaks at 1616 cm^{-1} and 1675 cm^{-1}. During the cocrystallization of TPH and NAM, because of the hydrogen bond formation, the characteristic peaks of TPH and NAM were found to shift to 1611 cm^{-1} and 1707 cm^{-1} [17]. The extrudates with polymeric carriers displayed a similar shift due to hydrogen bonding compared to the neat co-crystal. These results indicated the formation of the TPH-NAM co-crystal and were consistent with the reported data [17].

4.4. Powder X-Ray diffraction

The X-ray diffractograms of the physical mixture, pure components, and processed co-crystals are illustrated in Fig. 5. NAM displays characteristic peaks at 14.9 °C and 25.8 °C while TPH displays peaks at 20.3 °C and 22.7 °C [17]. The TPH NAM co-crystal revealed a characteristic peak at 13.4 °C, indicating the formation of a new phase during the extrusion processing of TPH and NAM. These results demonstrated the predominant nature of the co-crystal form in all extrudates. Further, the Kollidon® VA-64 assisted co-crystal exhibited a similar new peak at 13.4 °C, indicating co-crystal formation. The PXRD data supported the findings from DSC and FTIR studies. Thus, co-crystal formation was dependent on the non-covalent intermolecular hydrogen bonding interactions, thereby confirming the formation of

the co-crystal of NAM and TPH using the HME process. The presence of lower concentration of polymer (5% w/w) did not affect the nature of co-crystal formed.

4.5. Scanning Electron Microscopy

SEM showed differences in shape and size between the extruded co-crystals and pure components. As shown in Fig. 6, pure TPH has thin needle shaped crystals of bigger size and a regular shape with smooth surface while NAM has a rod-shaped crystalline structure. The co-crystals (Fig. 6C, F4) showed irregularity with an undistributed geometry with porous and rough surface, which might have resulted in the enhanced dissolution rate as compared to the pure TPH, suggesting a different crystal form than those of TPH and NAM. The size of the co-crystals was comparatively less than that of the pure components, which further supports the results of particle size distribution. Further, the SEM images of the polymer-assisted co-crystals (Fig. 6 D, E, F) revealed clumped, thin sticks and deformed shape with porous and hard surface. However the magnitude was comparatively less than that of the neat co-crystals.

4.6. Particle size distribution

The average particle size distribution of the milled extrudates for plain co crystal was predominantly in the range of sieve 60 and 80 whereas the polymeric assisted co-crystals (F5, F6, F7) was around sieve 60, 80 and 120), however the major portion of blend was around sieve 80 for all formulations. This suggested polymeric assisted co crystals produced relatively more fine portion than the plain co crystals. This demonstrates the type of mill and milling time plays an important role to control the particle size distribution of extrudates.

4.7. Pharmaceutical characterization

4.7.1. Carr's compressibility index and Hausner's ratio—The flow properties of TPH and the TPH NAM co-crystal with and without the incorporation of polymeric carriers were assessed by examining the bulk and tapped densities. The compressibility index and hausner's ratio data revealed that the TPH NAM co-crystal had a relatively better flow property than pure TPH. The compressibility index and hausner's ratio for the TPH NAM co-crystal was found to be 24.87 and 1.27 (passable), respectively, compared to pure TPH, which exhibited values of 29.25 and 1.41 (poor), respectively. Further, the extrudates with polymeric carriers also possessed good flow properties relative to pure TPH. The extrudates with HPMCAS-MG as a polymeric carrier demonstrated good flow property with a compressibility index of 14.34 and hausner's ratio of 1.15 (good). The compressibility index and hausner's ratio for the extrudates with PEO N80 as a polymeric carrier were 23.72 and 1.31 (passable), respectively. Lastly, the compressibility index and hausner's ratio for the Kollidon® VA-64 assisted co-crystals were 22.86 and 1.28 (passable), respectively. The flow characteristic of the tablet blend was observed to be passable compared to that of pure TPH. These findings suggested the relatively improved flow characteristics of the prepared pharmaceutical and polymer-assisted co-crystals.

4.8. Loss on drying

The observed loss on drying results indicated that the TPH NAM co-crystals had a consistently higher percentage of moisture content compared to that of pure TPH. The observed moisture content for pure TPH was 0.45% while that for TPH NAM co-crystals was comparatively higher at 0.76%; however, these observed values were less than 1%. Further, these results demonstrated the relatively increased hygroscopicity of TPH in the TPH NAM co-crystals [17]. These findings suggested that suitable packing and storage conditions must be established.

4.9. In vitro dissolution study

In vitro dissolution studies were performed to assess the performance of the co-crystals in comparison with pure TPH. The dissolution profiles for TPH and TPH NAM co-crystal in water awere shown in Fig. 7a. At 5 min, a drug release of 62.61 ± 1.53% was observed for pure TPH, while 68.18 ± 3.26% was observed for the TPH NAM co-crystal. Moreover, the drug release value from the TPH NAM co-crystal reached a maximum of 94.20 ± 4.16% while pure TPH showed a value of 85.64 ± 3.38% drug release at 15 min. Additionally, at 45 min, a plateau was achieved for both pure TPH and the TPH NAM co-crystal. These data demonstrate a directional difference between pure TPH and TPH NAM co-crystal at 3 time points of the release profile.

The dissolution profile of the co-crystals with the polymeric carriers PEO N80 and HPMCAS-MG is shown in Fig. 7a. Relatively, slow dissolution was observed for the polymer-based co-crystals, this may be due to binding of polymer with drug particles. Additionally, PEO (F6) had a comparatively higher drug release to that of the co-crystals suspended in HPMCAS-MG (F5), an enteric amorphous polymer. The highest dissolution rate of PEO was due to increased wetting of the co-crystals in the composites [29]. The relatively low dissolution of HPMCAS-MG processed co-crystals might be due to the impact of enteric nature or pH-dependent solubility of the HPMCAS-MG polymer. The dissolution data for the Kollidon VA-64® assisted co-crystals revealed a drug release of 83.95 ± 1.94% in 15 min (F7). This increased dissolution rate exhibited by the Kollidon VA-64® assisted co-crystals compared to HPMCAS-MG and PEO N80, is due to the enhanced solubilizing capacity of Kollidon VA-64®.

Lastly, the feasibility of the solid dosage formulation and its impact on the dissolution characteristics of the co-crystal tablets was investigated. A physical blend and compressed tablets were prepared to assess the impact of the compression force and the processability of the extruded co-crystals. The tablets were compressed using manual tablet compaction machine (Globe Pharma Inc, MTCM-I, NJ) with a tablet weight of 250 mg; a punch size of 8 mm at compression force of 300 psi and hardness of tablets was 3.11 ± 0.09. As shown in Fig. 7b, complete drug release was observed from the physical blend, co-crystal, and compressed tablet. However, the release from the tablet blend was complete in 5 min as compared to the extruded plain co-crystal and corresponding tablet. Complete drug release from all formulations was observed within the study period. These findings suggested the feasibility of formulating co-crystals into a solid dosage form.

4.10. Stability studies

Table 2 shows the enthalpy values of the DSC results for the formulations F4 and F7. Further, DSC thermograms are represented in Fig. 8. NAM polymorphs at 106 °C with enthalpy (ΔH) value of 1.247J/g were observed for the F4 formulation on the first day. Further, no such peak was observed at the stability conditions of 40 (±2) ° C/75 (±5) % RH for the study period. As reported in the literature, NAM has four polymorphs, the one at 106 °C is a metastable form and NAM displays polymorphic changes upon storage [30–32]. As seen in the DSC thermogram of Fig. 8 the initial sample showed characteristic peak, which may be attributed due to metastable form of NAM, which might be transformed into stable form during storage, because of which no characteristic polymorphic peak of NAM was observed in storage samples. Another noted observation was no NAM or TPH polymorphic peaks were observed in F7. Thus, the incorporation of an appropriate polymer (Kollidon VA64®) plays a vital role in processability. Further, it has been reported that PVP/VA polymers are a good candidate for intermolecular hydrogen bond interactions, with a small amount of 5% of polymer additive (VA-64) the prominent effect was noticed[33]. The DSC results indicated that the extrudates were stable and showed no degradation for three months in stability studies conducted at 40 (±2) ° C/75 (±5) % RH.

5. Conclusions

In this study, authors demonstrated the application of HME in the production of co-crystals for the model TPH NAM co-crystal system. Despite eutectic formation, extrusion was found to be an effective and viable method for developing co-crystals. The extrusion parameters that influenced co-crystal formation were extrusion temperature, screw design, and screw speed. Further, the use of an appropriate polymer was important in the processability and formation of stable co-crystals. The incorporation of polymer carriers such as HPMCAS-MG, PEO N80, and Kollidon® VA-64 in the extrusion process provided further flexibility in optimizing co-crystal production. The incorporation of the Kollidon® VA-64 polymer in the extrusion process led to co-crystal production without any eutectic formation and enabled the feasibility of formulating co-crystals into a solid dosage form. The three-month stability studies revealed no degradation and supported the rationale for the development of the TPH NAM co-crystal, since TPH is prone to hydrate formation during storage. Therefore, HME can be considered as an efficient, scalable, and solvent-free process for the manufacture of cocrystals, thereby providing a viable alternative to solution crystallization processes and other conventional techniques.

Acknowledgements

First author would like to thank Adwait Pradhan and Mittal Darji (Department of Pharmaceutics & Drug Delivery, University of Mississippi) for help in extrusion process. Scanning Electron Microscopy images presented in this work were generated using the instruments and services at the Microscopy and Imaging Center, The University of Mississippi. This facility is supported in part by grant 1726880, National Science Foundation.

Funding

This project was partially supported by Grant Number P30GM122733-01A1, funded by the National Institute of General Medical Sciences (NIGMS) a component of the National Institutes of Health (NIH) as one of its Centers of Biomedical Research Excellence (COBRE).

References

[1]. Patil H, Tiwari RV, Repka MA, Hot-melt extrusion: from theory to application in pharmaceutical formulation, AAPS PharmSciTech 17 (1) (2016) 20–42. [PubMed: 26159653]

[2]. Dumpa NR, et al., Chronotherapeutic drug delivery of ketoprofen and ibuprofen for improved treatment of early morning stiffness in arthritis using hot-melt extrusion technology, AAPS PharmSciTech 19 (6) (2018) 2700–2709. [PubMed: 29968041]

[3]. Krier F, et al., PAT tools for the control of co-extrusion implants manufacturing process, Int. J. Pharm. 458 (1) (2013) 15–24. [PubMed: 24148661]

[4]. Pimparade MB, et al., Development of taste masked caffeine citrate formulations utilizing hot melt extrusion technology and in vitro-in vivo evaluations, Int. J. Pharm. 487 (1–2) (2015) 167–176. [PubMed: 25888797]

[5]. Gryczke A, et al., Development and evaluation of orally disintegrating tablets (ODTs) containing Ibuprofen granules prepared by hot melt extrusion, Colloids Surf. B Biointerfaces 86 (2) (2011) 275–284. [PubMed: 21592751]

[6]. Roblegg E, et al., Development of sustained-release lipophilic calcium stearate pellets via hot melt extrusion, Eur. J. Pharm. Biopharm 79 (3) (2011) 635–645. [PubMed: 21801834]

[7]. Bhagurkar AM, et al., Development of an ointment formulation using hot-melt extrusion technology, AAPS PharmSciTech 17 (1) (2016) 158–166. [PubMed: 26628438]

[8]. Cosse A, et al., Hot melt extrusion for sustained protein release: matrix erosion and in vitro release of PLGA-based implants, AAPS PharmSciTech 18 (1) (2017) 15–26. [PubMed: 27193002]

[9]. Kallakunta VR, et al., Effect of formulation and process variables on lipid based sustained release tablets via continuous twin screw granulation: a comparative study, Eur. J. Pharmaceut. Sci. 121 (2018) 126–138.

[10]. LaFountaine JS, McGinity JW, Williams RO 3rd, Challenges and strategies in thermal processing of amorphous solid dispersions: a review, AAPS PharmSciTech 17 (1) (2016) 43–55. [PubMed: 26307759]

[11]. Saerens L, et al., In-line NIR spectroscopy for the understanding of polymer-drug interaction during pharmaceutical hot-melt extrusion, Eur. J. Pharm. Biopharm. 81 (1) (2012) 230–237. [PubMed: 22269939]

[12]. Wesholowski J, et al., Scale-Up of pharmaceutical Hot-Melt-Extrusion: process optimization and transfer, Eur. J. Pharm. Biopharm. 142 (2019) 396–404. [PubMed: 31295504]

[13]. Repka MA, et al., Applications of hot-melt extrusion for drug delivery, Expet Opin. Drug Deliv 5 (12) (2008) 1357–1376.

[14]. Bolla G, Nangia A, Pharmaceutical cocrystals: walking the talk, Chem Commun (Camb) 52 (54) (2016) 8342–8360. [PubMed: 27278109]

[15]. Qiao N, et al., Pharmaceutical cocrystals: an overview, Int. J. Pharm. 419 (1–2) (2011)1–11. [PubMed: 21827842]

[16]. Witika BA, Smith VJ, Walker RB, Quality by design optimization of cold sonochemical synthesis of zidovudine-lamivudine nanosuspensions, Pharmaceutics 12 (4) (2020).

[17]. Lu J, Rohani S, Preparation and characterization of theophylline– nicotinamide cocrystal, Org. Process Res. Dev. 13 (6) (2009) 1269–1275.

[18]. Karimi-Jafari M, et al., Creating cocrystals: a review of pharmaceutical cocrystal preparation routes and applications, Cryst. Growth Des. 18 (10) (2018) 6370–6387.

[19]. Repka MA, et al., Melt extrusion with poorly soluble drugs-An integrated review, Int. J. Pharm. 535 (1–2) (2018) 68–85. [PubMed: 29102700]

[20]. Daurio D, et al., Application of twin screw extrusion in the manufacture of cocrystals, part I: four case studies, Pharmaceutics 3 (3) (2011) 582–600. [PubMed: 24310598]

[21]. Li S, et al., Mechanochemical synthesis of pharmaceutical cocrystal suspensions via hot melt extrusion: feasibility studies and physicochemical characterization, Mol. Pharm. 13 (9) (2016) 3054–3068. [PubMed: 27314248]

[22]. Li S, et al., Mechanochemical synthesis of pharmaceutical cocrystal suspensions via hot melt extrusion: enhancing cocrystal yield, Mol. Pharm. 15 (9) (2018) 3741–3754. [PubMed: 29166563]

[23]. Ervasti T, Aaltonen J, Ketolainen J, Theophylline-nicotinamide cocrystal formation in physical mixture during storage, Int. J. Pharm. 486 (1–2) (2015) 121–130. [PubMed: 25800677]

[24]. Douroumis D, Ross SA, Nokhodchi A, Advanced methodologies for cocrystal synthesis, Adv. Drug Deliv. Rev. 117 (2017) 178–195. [PubMed: 28712924]

[25]. Tiwari R, et al., Formulation and evaluation of sustained release extrudes prepared via novel hot melt extrusion technique, Journal of Pharmaceutical Innovation 9 (3) (2014) 246–258.

[26]. Boksa K, Otte A, Pinal R, Matrix-assisted cocrystallization (MAC) simultaneous production and formulation of pharmaceutical cocrystals by hot-melt extrusion, J. Pharmaceut. Sci 103 (9) (2014) 2904–2910.

[27]. Gajda M, et al., Tuning the cocrystal yield in matrix-assisted cocrystallisation via hot melt extrusion: a case of theophylline-nicotinamide cocrystal, Int. J. Pharm. 569 (2019) 118579. [PubMed: 31362095]

[28]. Kallakunta VR, et al., Exploratory studies in heat-assisted continuous twin-screw dry granulation: a novel alternative technique to conventional dry granulation, Int. J. Pharm. 555 (2019) 380–393. [PubMed: 30458256]

[29]. Gajda M, et al., The role of the polymer matrix in solvent-free hot melt extrusion continuous process for mechanochemical synthesis of pharmaceutical cocrystal, Eur. J. Pharm. Biopharm. 131 (2018) 48–59. [PubMed: 30205892]

[30]. Li J, Bourne SA, Caira MR, New polymorphs of isonicotinamide and nicotinamide, Chem Commun (Camb) 47 (5) (2011) 1530–1532. [PubMed: 21088781]

[31]. Bucar DK, Lancaster RW, Bernstein J, Disappearing polymorphs revisited, Angew Chem. Int. Ed. Engl. 54 (24) (2015) 6972–6993. [PubMed: 26031248]

[32]. Hino T, Ford JL, Powell MW, Assessment of nicotinamide polymorphs by differential scanning calorimetry, Thermochim. Acta 374 (1) (2001) 85–92.

[33]. Browne E, Worku ZA, Healy AM, Physicochemical properties of poly-vinyl polymers and their influence on ketoprofen amorphous solid dispersion performance: a polymer selection case study, Pharmaceutics 12 (5) (2020) 433.

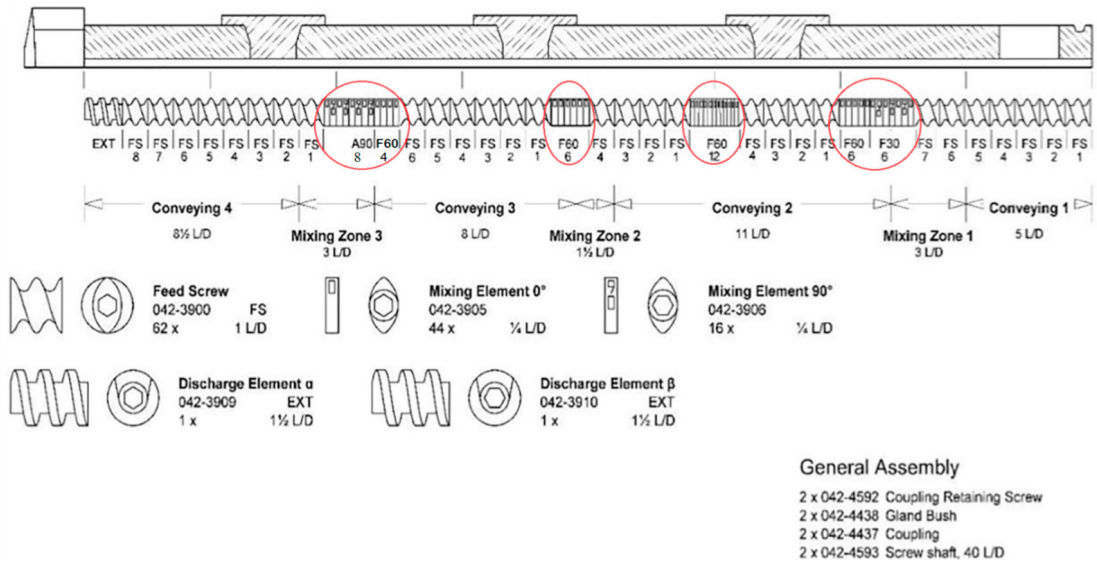

Fig 1.

Schematic illustration of the customized screw configuration with an 11-mm extruder.

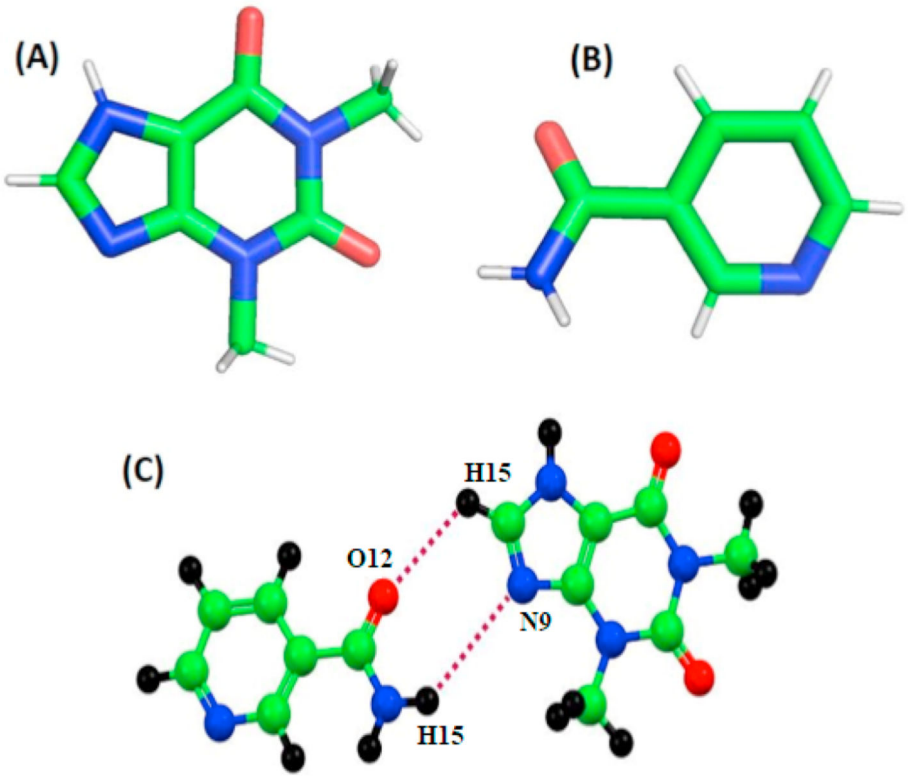

Fig 2.

(A) Theophylline (TPH) structure, (B) Nicotinamide (NAM) structure, and (C) Intermolecular hydrogen bond between TPH and NAM.

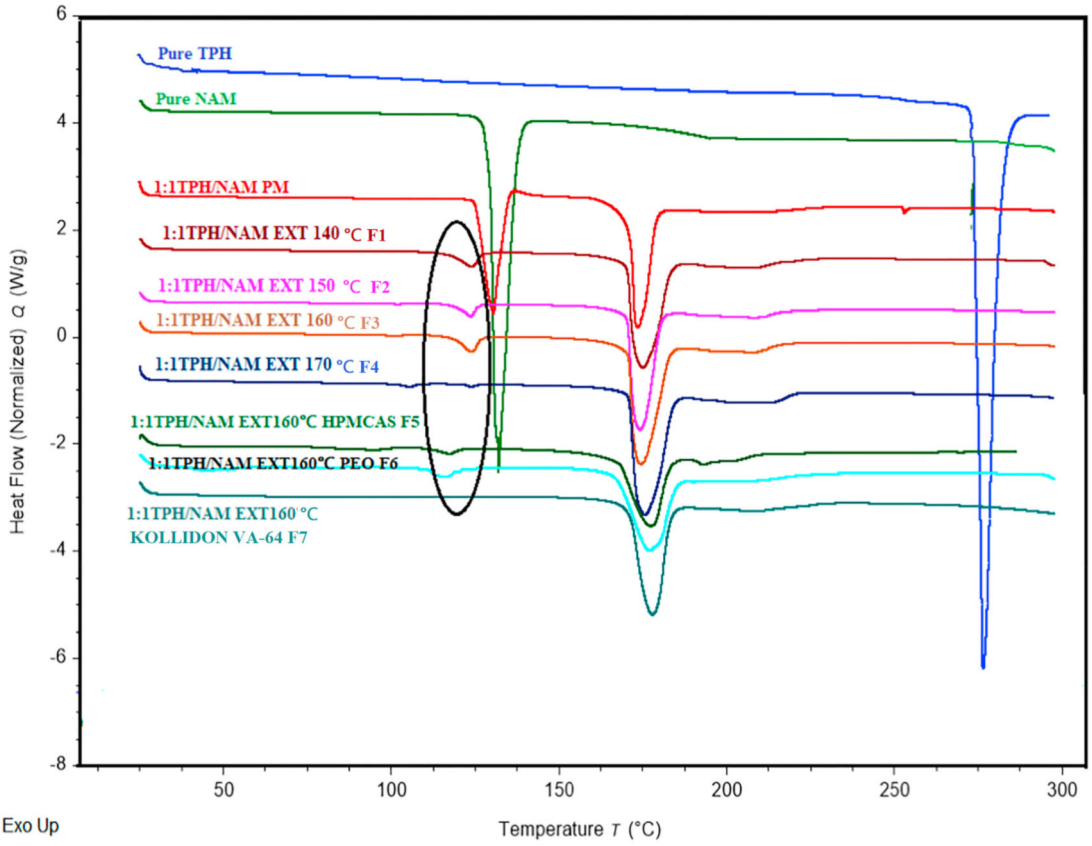

Fig 3.

DSC thermograms of pure theophylline, pure nicotinamide, physical mixture (PM), and extrudates at different temperatures.

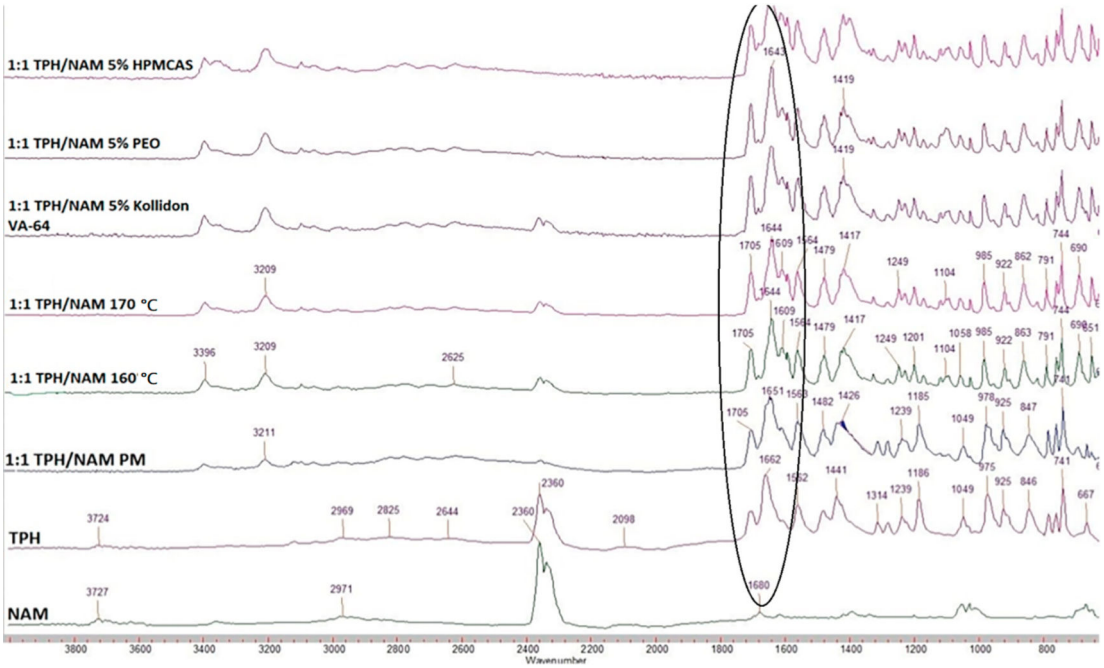

Fig 4.

FTIR spectra of pure theophylline, pure nicotinamide, physical mixture (PM), and extrudates at different temperatures.

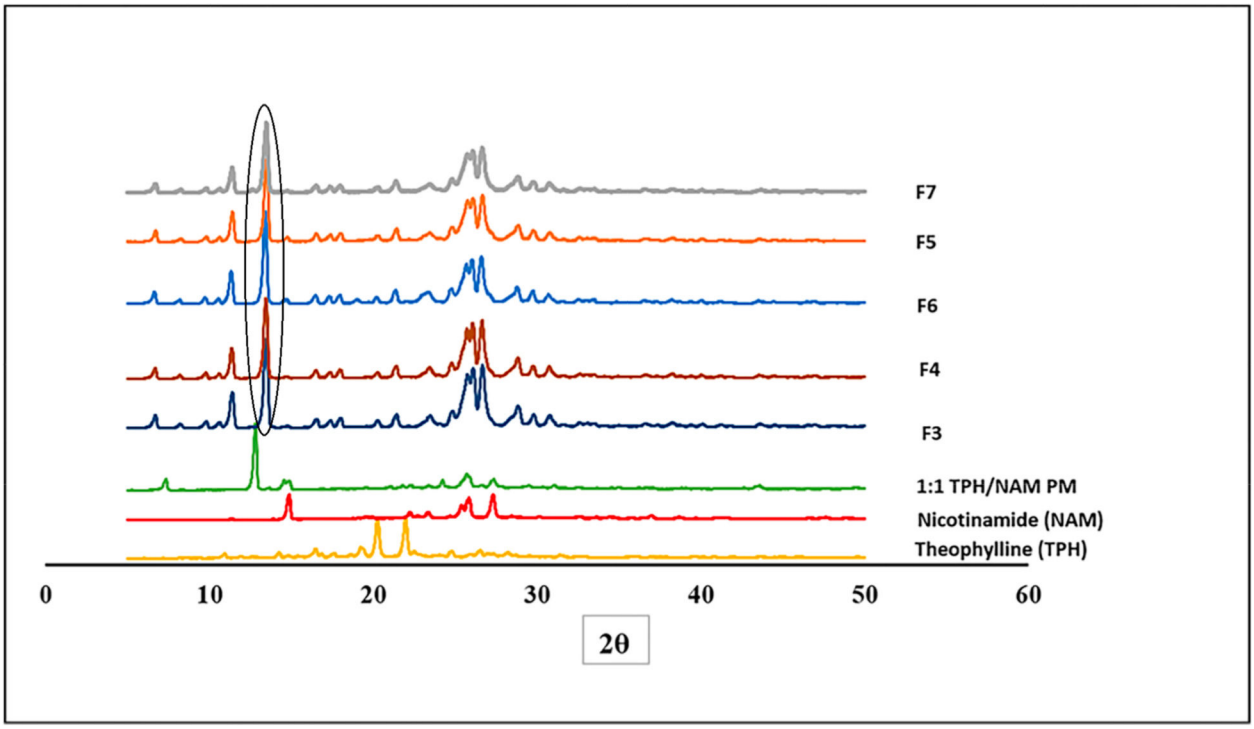

Fig 5.
PXRD diffractograms of pure theophylline, pure nicotinamide, physical mixture (PM), and extrudates.

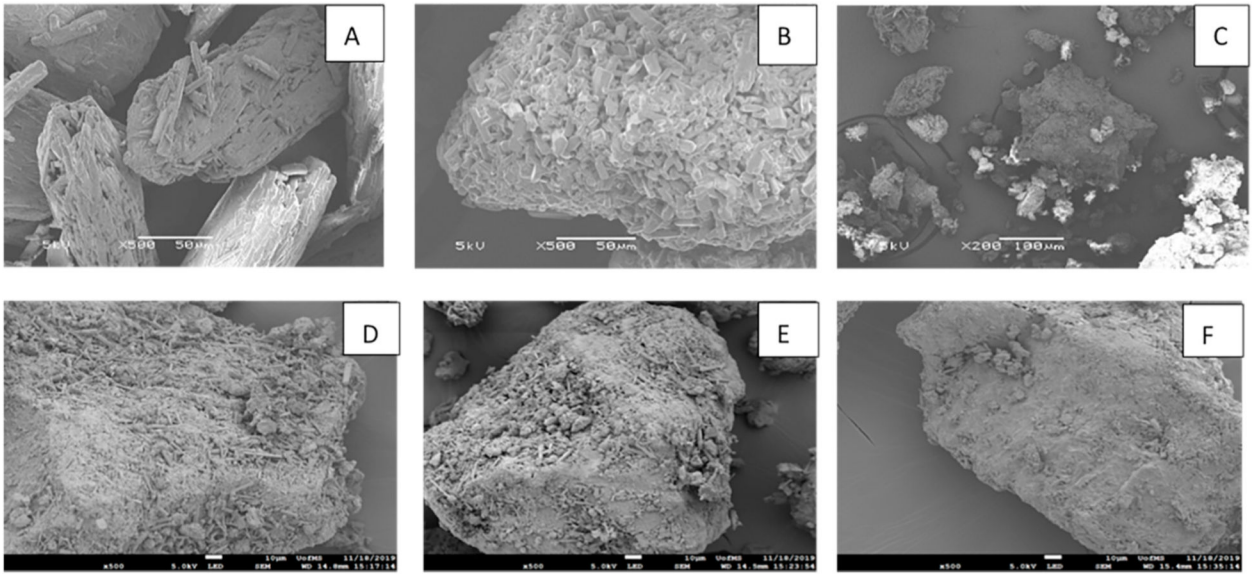

Fig 6.

Scanning electron microscopy (SEM) images of (A) pure theophylline, (B) pure nicotinamide, (C) 1:1 Theophylline Nicotinamide 170 ° C (F4) extrudates, (D) 1:1 Theophylline Nicotinamide with 5% HPMCAS-MG (F5), (E) 1:1 Theophylline Nicotinamide with 5% PEO (F6), and (F) 1:1 Theophylline Nicotinamide with 5% Kollidon® VA-64 (F7).

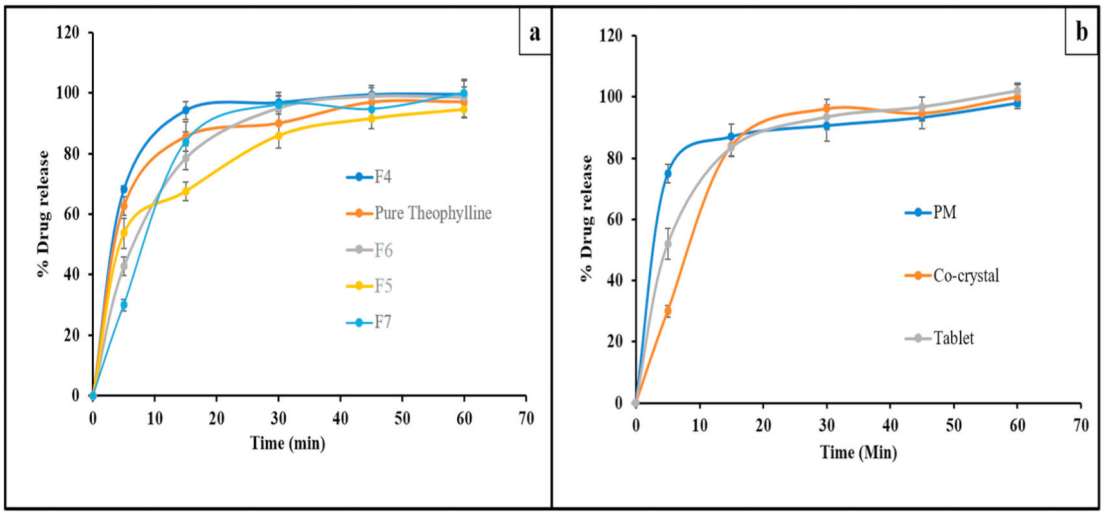

Fig 7.

In vitro drug release profiles of (a) pure theophylline and extrudates, (b) physical blend (PM), co-crystal and compressed tablet.

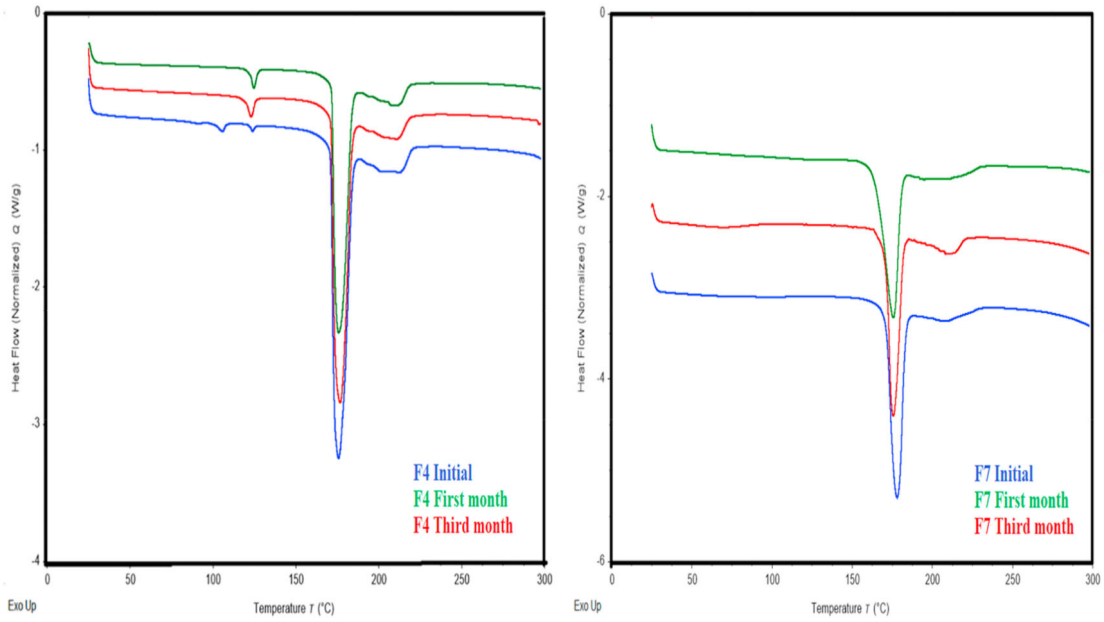

Fig 8.

DSC thermograms of 1:1 theophylline nicotinamide 170 °C (F4) and 1:1 theophylline nicotinamide with 5% Kollidon® VA-64 (F7) extrudates on the first day, first month, and third month at 40 (±2) °C and 75 (±5) % RH.

Table 1

Formulation compositions, processing parameters, and the observation of co-crystal formation during the HME process.

Formulation	Processing Temp. (°C)	Screw Speed (Rpm)	Torque (%)	Observation
1:1 TPH NAM (F1)	140	50	42–48	Eutectic peak was observed at 126.4 °C. Fine agglomerates
1:1 TPH NAM (F2)	150	50	45–51	Eutectic peak was observed at 126.4 °C. Fine agglomerates
1:1 TPH NAM (F3)	160	50	50–58	Eutectic peak was observed at 126.4 °C. Fine agglomerates
1:1 TPH NAM (F4)	170	50	50–58	Eutectic peak was observed at 126.4 °C with decreased intensity. Fine agglomerates
1:1 TPH NAM with 5% HPMCAS-MG (F5)	160	50	35–42	DSC thermogram with eutectic peak similar to the neat co-crystal was observed. Extrudate strands were produced
1:1 TPH NAM with 5% PEO (F6)	160	50	40–45	DSC thermogram with eutectic peak similar to the neat co-crystal was observed. Extrudate strands were produced
1:1 TPH NAM with 5% Kollidon VA-64 (F7)	160	50	25–30	Eutectic peak at 126.4 °C was disappeared and complete co-crystal formation at 174 °C was observed. Extrudate strands were produced

Table 2

Comparison of the thermal data for F4 and F7 formulations for the accelerated stability conditions (40 (±2) °C and 75 (±5) % RH).

Time	F4		F7	
	Eutectic peak (Enthalpy J/g)	Co-crystal peak (Enthalpy J/g)	Eutectic peak (Enthalpy J/g)	Co-crystal peak (Enthalpy J/g)
Initial	1.610	119.56	No eutectic 101.78	
First month	4.142	110.83	No eutectic 114.43	
Third month	3.016	107.95	No eutectic 103.54	